Photochemical evolution of organic aerosols observed in urban plumes from Hong Kong and the Pearl River Delta of China

CrossMark

Shengzhen Zhou [a,b], Tao Wang [a,b,*], Zhe Wang [b], Weijun Li [a], Zheng Xu [a,b], Xinfeng Wang [a], Chao Yuan [a], C.N. Poon [b], Peter K.K. Louie [c], Connie W.Y. Luk [c], Wenxing Wang [a,d]

[a] Environment Research Institute, Shandong University, Ji'nan, Shandong 250100, PR China
[b] Department of Civil and Environmental Engineering, The Hong Kong Polytechnic University, Hong Kong, PR China
[c] Environmental Protection Department, Government of the Hong Kong Special Administrative Region, Hong Kong, PR China
[d] Chinese Research Academy of Environmental Sciences, Beijing 100012, PR China

HIGHLIGHTS

- Hourly measurements of carbonaceous aerosols in Hong Kong are presented in this paper.
- Photochemical evolutions of organic aerosols were examined during the photochemical episodes.
- The SOC production rates ranged from 1.31 to 3.86 $\mu g\ m^{-3}\ ppmv^{-1}\ h^{-1}$.
- Thick organic coatings were internally mixed with inorganic sulfate/nitrate in the aged plumes.

ARTICLE INFO

ABSTRACT

Organic aerosols influence human health and global radiative forcing. However, their sources and evolution processes in the atmosphere are not completely understood. To study the aging and production of organic aerosols in a subtropical environment, we measured hourly resolved organic carbon (OC) and element carbon (EC) in PM$_{2.5}$ at a receptor site (Tung Chung, TC) in Hong Kong from August 2011 to May 2012. The average OC concentrations exhibited the highest values in late autumn and were higher during the daytime than at night. The secondary organic carbon (SOC) concentrations, which were estimated using an EC-tracer method, comprised approximately half of the total OC on average. The SOC showed good correlation with odd oxygen ($O_x = O_3 + NO_2$) in the summer and autumn seasons, suggestive of contribution of photochemical activities to the formation of secondary organic aerosols (SOA). We calculated production rates of SOA using the photochemical age (defined as $-Log_{10}(NO_x/NO_y)$) in urban plumes from the Pearl River Delta (PRD) region and Hong Kong during pollution episodes in summer and autumn. The CO-normalized SOC increased with the photochemical age, with production rates ranging from 1.31 to 1.82 $\mu g\ m^{-3}\ ppmv^{-1}\ h^{-1}$ in autumn and with a larger rate in summer (3.86 $\mu g\ m^{-3}\ ppmv^{-1}\ h^{-1}$). The rates are in the range of the rates observed in the outflow from Mexico City, the eastern U.S. and Los Angeles. Microscopic analyses of the individual aerosol particles revealed large contrasts of aerosol physico-chemical properties on clean and smoggy days, with thick organic coatings internally mixed with inorganic sulfate for all particle sizes in the aged plumes from the PRD region.

© 2014 Elsevier Ltd. All rights reserved.

1. Introduction

Carbonaceous aerosols, which are composed of organic carbon (OC) and element carbon (EC, also termed black carbon or soot), have significant effects on global climate and human health (Nel, 2005; Bond et al., 2013). OC can be either directly emitted from primary combustion sources together with EC (primary OC, POC) or formed through the gas-particle conversion of reactive organic gas

oxidation and atmospheric heterogeneous reactions (secondary OC, SOC) (Seinfeld and Pandis, 2006). EC is emitted from incomplete combustions, such as biomass burning and fossil fuel combustion.

Recent studies have indicated that secondary organic aerosols (SOA) account for 63–95% of the organic aerosols (OA) in urban, rural, and remote sites (Zhang et al., 2007b), and the POC can be further oxidized to SOC after emission (Robinson et al., 2007). Although substantial efforts have been made in understanding SOA formation, their sources and atmospheric evolution processes remain inadequately characterized (Jimenez et al., 2009). The current air quality models, which are mainly based on the parameters defined by laboratory experiments, cannot represent the magnitudes and evolution of organic aerosols in the real atmosphere (Jimenez et al., 2009), and the mass of modeled and measured organic aerosols were not always agreed (Johnson et al., 2006; Dzepina et al., 2010).

Urban areas act as the sources of aerosols and aerosol precursors (e.g., SO_2, NO_x, volatile organic compounds (VOCs)). Secondary aerosols are produced from the oxidation of such precursors, and both primary aerosols and secondary aerosols undergo atmospheric processes within and downwind of the source regions. Field studies have been conducted to investigate the processing of aerosols in urban centers and their surrounding areas, such as in Mexico City (Kleinman et al., 2008; Jimenez et al., 2009; DeCarlo et al., 2010), the northeastern U.S. (De Gouw et al., 2008), the southern and southeastern U.S. (Weber et al., 2007; Bahreini et al., 2009), Tokyo (Miyakawa et al., 2008), Ontario (Slowik et al., 2011), and California (Hayes et al., 2013). These studies have shown the amount of SOA to be several times that of the initial primary organic aerosol concentration after a few hours of photochemical aging.

The Pearl River Delta region (PRD region, including the cities of Guangzhou, Shenzhen, Dongguan, Foshan, Jiangmen, Zhongshan and Zhuhai, and the urban areas of Huizhou and Zhaoqing) is situated in the central southern part of Guangdong Province alongside the Pearl River Estuary (Fig. 1). It is one of the most urbanized and industrialized areas in China. Although the PRD region covers only 0.5% of China's total land area and holds about 4% of its total population, its gross domestic product comprised about 14% of China's total in 2010 (Zhong et al., 2013). Along with rapid economic and population growth, the PRD region and adjacent Hong Kong (HK) metropolitan area suffer from severe photochemical smog pollution and high concentrations of fine particles (Chan and Yao, 2008; Zhang et al., 2008b; Wang et al., 2009). As one of the major components of submicron aerosols, carbonaceous aerosols have been studied intensively in HK-PRD region. Some topics of carbonaceous aerosols have been well investigated, such as the spatio-temporal distributions of mass concentrations (Cao et al., 2004; Yu et al., 2004; Hagler et al., 2006), size distributions (Huang et al., 2006; Gnauk et al., 2008; Yu et al., 2010), optical properties (Cheng et al., 2006; Andreae et al., 2008), source identifications (Zheng et al., 2011) and apportionment of primary and secondary organic aerosols (Yuan et al., 2006; Hu et al., 2010; Ding et al., 2012). These studies were mostly based on an integrated filter sampling method with a low time resolution (hours or days) and thus could not quantify the chemical processing of carbonaceous aerosols occurring on a short time scale. Recently, several field studies have reported the measurement results of carbonaceous aerosols using high-resolution instruments in the HK-PRD region. With a quadrupole aerosol mass spectrometer, Xiao et al. (2009) observed good correlation between a SOA tracer (i.e., m/z 44) and sulfate in the condensation mode in July 2006 in the PRD outflow and suggested that SOA was formed from the gas-phase oxidation of VOCs. Hu et al. (2012) studied the temporal variation of carbonaceous aerosols at a rural site of the PRD (Back Garden) in July 2006 and quantified the POC and SOC using a modified EC-tracer method with a semi-continuous thermal-optical OC/EC analyzer. Lee et al. (2013) reported size-resolved chemical compositions of the non-refractory submicron aerosol species (including organics) using a HR-ToF-AMS in Hong Kong in May 2011.

During August 2011–May 2012, we conducted a comprehensive field study in select months at a suburban Hong Kong site that frequently received plumes from the urban areas of Hong Kong and the PRD. This paper presents its findings on hourly resolved carbonaceous aerosols together with other relevant chemical data and aerosol morphology. Compared with the previous work on carbonaceous aerosols, our study was unique in that (1) it made
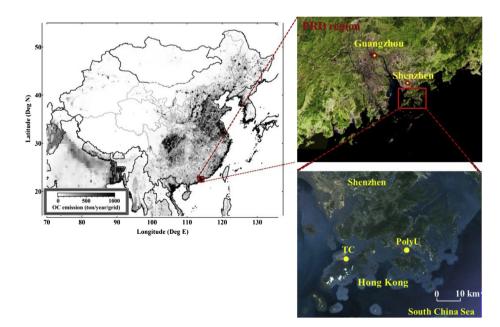

Fig. 1. Map of China and locations of the sampling sites in Hong Kong: a receptor site in Tung Chung (TC, 22.289°N, 113.943°E) and an urban site on the campus of the Hong Kong Polytechnic University (PolyU, 22.303°N, 114.179°E). The girded Asia OC emissions in 2006 are also shown (http://mic.greenresource.cn/intex-b2006).

hourly resolved trace gases and aerosol compositions concurrently available, enabling us to quantify photochemical age and thus the production rates of SOC in a polluted subtropical environment, and (2) aerosol morphology information was examined together with bulk aerosol chemical data. We began by introducing abundances and seasonal/diurnal variations of carbonaceous aerosols, and estimated the fraction of SOC using an EC-tracer method with the aid of other information on photochemical age and biomass burning tracers. We then focused on examining the production rates of SOC in individual urban plumes from Hong Kong and the PRD region, and finally investigated the mixing state of organic aerosol using transmission electron microscope (TEM). This multi-technique approach led to an improved understanding of the sources and formation of carbonaceous aerosols in the outflow from sub-tropical urban and industrial regions.

2. Experimental

2.1. Sampling location and periods

Hong Kong is located on the eastern side of the Pearl River Estuary on the South China coast. Its climate is governed by the Asian monsoons. The prevailing synoptic winds are the northerlies and north-easterlies in winter, the easterlies in spring and autumn and the southwesterlies in summer (Wang et al., 2001). Our measurement site was located at Tung Chung (TC, 22.289°N, 113.943°E) on Lantau Island southwest of Hong Kong. TC is a new town with a population of approximately 80,000, and Che Lap Kok International Airport is located 3 km to the north of the site. The sampling inlet of carbonaceous aerosols was placed on the rooftop of a health center in the town. The site is unique in that it is surrounded by the region's major urban areas (Wang et al., 2001). The measurements were conducted in 4 non-consecutive months: August 3–September 7, 2011 in late summer; November 1–December 3, 2011 in late autumn; February 18–March 9, 2012 in late winter and May 1–31, 2012 in late spring.

2.2. Measurement instruments

The OC and EC concentrations in $PM_{2.5}$ were measured hourly using an in-situ semi-continuous OC and EC analyzer (Dual-Oven Model, Sunset Laboratory Inc., USA). Wang et al. (2011) presented a detailed description of the instrument's principle and operation. In this study, a 1-h measurement cycle was used, with 43 min devoted to sampling and 17 min to analysis during the summer, autumn and winter measurements. A 2-h cycle with 103 min devoted to sampling and the remaining time to analysis was used for the spring measurement due to the low aerosol mass concentrations. The detection limit for OC and EC was 0.3 and 0.1 μg m^{-3}, respectively (Wang et al., 2011).

A suite of trace gases was measured continuously during the field study, including $NO/NO_2/NO_x$ (TEI, Model 42i with a blue light converter), NO_y (TEI, Model 42i-Y), CO (TEI, Model 48C), O_3 (Teledyne, API 400), and SO_2 (TEI, Model 43A). Wang et al. (2003) and Xu et al. (2013) provided detailed information on these trace-gas analyzers. An ambient ion monitor (AIM, Model URG-9000B, USA) was applied to measure the hourly concentrations of water soluble inorganic ions, including SO_4^{2-}, NO_3^-, Cl^-, NH_4^+, Na^+, K^+, Mg^{2+} and Ca^{2+} (Gao et al., 2012). In addition, hourly mass concentration of $PM_{2.5}$ was measured using a tapered element oscillating microbalance (TEOM 1405-DF, Thermo Scientific) with a Filter Dynamic Measurement System (FDMS).

Individual aerosol particles were also collected onto the carbon-film-coated copper TEM grids (carbon type-B, 300-mesh copper, Tianld Co., China) using a single-stage cascade impactor with a jet nozzle 0.5 mm in diameter at a flow rate of 1.0 l min^{-1} (Li et al.,

2013). The collected individual aerosol samples were analyzed using a high-resolution transmission electron microscope (TEM, JEOL JEM-2100) operated at 200 kV to determine the morphology, size and the mixing state of the individual aerosol particles. An energy-dispersive X-ray spectrometer (EDS) was used to obtain the compositions of the targeted particles.

2.3. EC-tracer method and photochemical age

2.3.1. EC-tracer method

The EC-tracer method has widely been used to estimate SOC concentrations due to its simplicity (Turpin and Huntzicker, 1995). The key step of this method is to determine the primary OC/EC ratio in the study period and region. In previous studies, the minimum OC/EC ratio or the lowest 5–10% OC/EC ratios have been applied as the primary OC/EC ratio (Lim and Turpin, 2002; Zhang et al., 2008a). In this present study, we made use of highly time-resolved measurements of the OC and EC and simultaneous, continuous measurements of other gas-phase and aerosol pollutants to determine the primary OC/EC ratio. We selected a subset of the data to represent primary OC and EC: that is, the data corresponding to the lowest 25% OC/EC ratios and the lowest 25% of O_3 concentrations in each season. The above selected data were subject to additional checks. We used the NO_x/NO_y ratio, which is an indicator of photochemical aging, to verify the primary OC and EC data. The results showed that the NO_x/NO_y ratios corresponding to the primary OC/EC data in each season were much higher (>0.92) than the respective monthly average ratio (summer: 0.78, autumn: 0.79, winter: 0.89, and spring: 0.84), indicating that the emissions during the selected periods were fresher. The EC-tracer method has an intrinsic drawback when a constant primary OC/EC ratio is adopted. Ding et al. (2012) reported that the EC-tracer method might have overestimated the SOC concentrations in the PRD region during the fall-winter biomass burning events, when high primary OC/EC ratios (>7) were observed. Therefore, we excluded the OC and EC data that could have been affected by biomass burning according to certain criteria (i.e., OC/EC ratios over 7 and obvious enhancement of potassium ion, a commonly used biomass burning tracer). In this study, 2% and 1% of the OC and EC data were excluded in summer and spring respectively, and no data were excluded during autumn and winter based on the criteria. This suggests that biomass burning had a minor influence on the TC site during our observation periods. The 'final' primary OC/EC ratio was derived through a linear regression of the selected sub data points. Since the source emission intensities and meteorological factors were different between the daytime (7:00–18:00) and nighttime (19:00–6:00), we derived the primary OC/EC ratios separately for daytime and nighttime.

2.3.2. Photochemical age

The NO_x/NO_y ratio has often been used as a photochemical 'clock' to help quantify the atmospheric evolution of organic aerosols (Kleinman et al., 2008; Miyazaki et al., 2009; Slowik et al., 2011; Wang et al., 2012). NO_x is emitted mostly as NO and then converted to NO_2 by rapidly reacting with O_3. Further oxidation of NO_2 leads to the formation of higher oxidation state compounds, and NO_y is the sum of NO_x and its oxidation products. As suggested by Kleinman et al. (2008), the photochemical age is defined as $-\log_{10}(NO_x/NO_y)$:

$$\int \kappa[OH]dt = -2.303 \log_{10}(NO_x/NO_y) = -\ln(NO_x/NO_y) \quad (1)$$

where κ is the rate constant of NO_2 reacting with OH, with a value about 7.9×10^{-12} molecules^{-1} cm^3 s^{-1} at 1 atm and 300 K (Slowik et al., 2011). [OH] is the average daytime OH radical
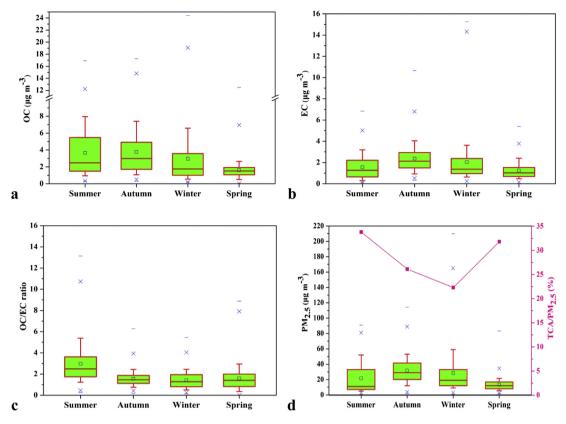
Fig. 2. Seasonal variations of (**a**) OC, (**b**) EC, (**c**) OC/EC ratio and (**d**) PM$_{2.5}$ and TCA/PM$_{2.5}$ ratio at TC. The squares denote the mean concentrations. The whiskers denote the 10th and 90th percentiles. "×" and "−" represent the 99th percentile and maximum and 1st percentile and minimum, respectively.
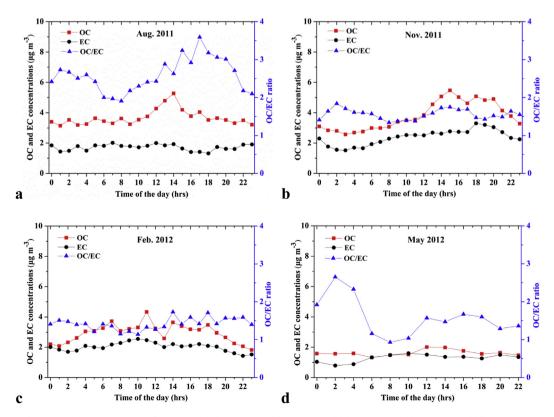

Fig. 3. Mean diurnal variations of OC, EC and OC/EC at TC in (**a**) late summer, (**b**) late autumn, (**c**) late winter and (**d**) late spring.

Table 1
Statistics of the estimated SOC concentrations during the four seasons in Tung Chung (TC), Hong Kong. σ stands for standard deviation.

Season	$(OC/EC)_{pri}$		SOC ($\mu g\ m^{-3}$)		SOC/OC (%)	
	Day	Night	Day (Mean ± σ)	Night (Mean ± σ)	Day (Mean ± σ)	Night (Mean ± σ)
Summer	1.35	1.72	2.77 ± 2.35	1.77 ± 1.30	46.9 ± 19.4	32.8 ± 18.8
Autumn	0.90	1.11	2.28 ± 2.50	1.41 ± 1.47	41.0 ± 17.5	32.5 ± 18.0
Winter	0.65	0.73	2.23 ± 2.73	1.58 ± 1.69	51.2 ± 20.2	48.9 ± 20.7
Spring	0.55	0.56	1.17 ± 1.12	1.01 ± 0.49	58.3 ± 18.4	62.1 ± 20.4

concentration, which is about 5.2×10^6 molecules cm^{-3} and 1.6×10^6 molecules cm^{-3} modeled at the TC site in summer and autumn, respectively (Wu et al., manuscript under preparation). The summer average daytime OH concentration at TC is comparable with the summer values of 4.0×10^6 molecules cm^{-3} in Tokyo (Miyakawa et al., 2008) and 3.6×10^6 molecules cm^{-3} in Ontario (Slowik et al., 2011); the autumn OH concentration is comparable with the 1.3×10^6 molecules cm^{-3} in California during the 2010 CalNex Campaign (Hayes et al., 2013) and the 1.6×10^6 molecules cm^{-3} in Mexico City (DeCarlo et al., 2010). At TC, the photochemical ages (i.e. $-Log_{10}(NO_x/NO_y)$) of 0.1, 0.4 and 0.8 were approximately 1.6, 6.2 and 12.5 h in summer and 5, 20 and 40 h in autumn, respectively. The longer times in the autumn season are due to smaller OH concentrations but comparable NO_x/NO_y ratios in summer and autumn. The uncertainty in using the above photochemical age has been investigated previously (Kleinman et al., 2008; Hayes et al., 2013). They point out that the NO_x emission sources are spatially distributed, which may revert the NO_x/NO_y ratio during the transport. As a result, this method may underestimate the photochemical ages, especially for the more aged plumes.

3. Results and discussion

3.1. Seasonal and diurnal variations of carbonaceous aerosols

Fig. 2 presents the seasonal variations of the mean mass concentrations of OC, EC and $PM_{2.5}$ and the OC/EC ratios. The average OC concentrations were 3.66, 3.76, 2.94 and 1.62 $\mu g\ m^{-3}$ in summer, autumn, winter and spring, respectively, with an annual mean concentration of 3.00 $\mu g\ m^{-3}$. The EC and $PM_{2.5}$ showed similar seasonal patterns, with the highest concentrations in autumn, followed by summer, winter and spring. The OC/EC ratio reached its highest value in summer, and the ratios in the other 3 months did not vary greatly. The total carbonaceous aerosol mass concentrations (TCA, TCA = $1.6 \times$ OC + EC) accounted for about one third of the $PM_{2.5}$ mass at TC (Fig. 2d).

The diurnal variations of the OC and EC concentrations and the OC/EC ratios in $PM_{2.5}$ in the four seasons are illustrated in Fig. 3. The EC showed high concentrations during the morning and evening rush hours, and the concentrations either dropped slightly (in summer, winter and spring) or kept a constant high level (in autumn) in the afternoon due to a deeper planetary boundary layer. The OC peaked in the noon or early afternoon, similar to the diurnal pattern of O_3 (Wang et al., 2001). This result suggests that the formation of O_3 and organic aerosols may have experienced the same photochemical process. Fig. 3 shows the afternoon peaks of the OC/EC ratio suggesting that SOC was formed through the daytime photochemical processes.
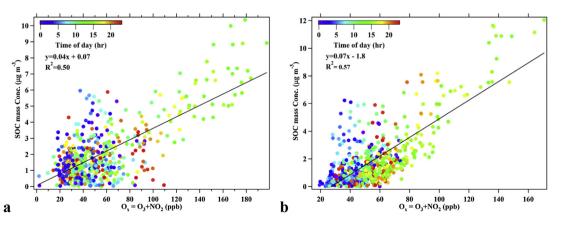
3.2. Estimation of SOC concentrations

Table 1 shows the calculated primary OC/EC ratios, the estimated mean SOC concentrations, and the contributions of SOC to the OC in the four seasons. The estimated primary OC/EC ratio in our study is 1.35, 0.9, 0.65, and 0.55 in daytime and 1.72, 1.11, 0.73, and 0.56 in nighttime in summer, autumn, winter, and spring, respectively. These ratios are similar to the value (0.6) observed in a tunnel in Hong Kong (Cheng et al., 2010), whereas our summer ratio is somewhat larger which may be due to stronger evaporative and biogenic emissions at high temperature. The SOC concentration was the highest in summer, followed by that in winter, autumn and spring. The daytime SOC concentrations were normally higher than those in the nighttime in all four seasons. Strong correlations between the SOC and odd oxygen ($O_x = O_3 + NO_2$) were observed in the summer and autumn seasons (Fig. 4), indicating that profound photochemical production of SOC in these two seasons. The SOC concentration in winter was comparable with that in autumn, a similar result to that of Yuan et al. (2006). Overall, the SOC concentrations accounted for about 47% of the total measured OC concentrations at TC, which is generally consistent with the previous work performed in Hong Kong (46%) for 1998–2002 (Yuan et al., 2006) and at a rural site (Back Garden) in the PRD region (47%) during the summer 2006 (Hu et al., 2012). The SOC to OC ratio was the largest in spring, followed by that in winter, summer and autumn.

3.3. Photochemical evolution and SOC formation in summer and autumn

3.3.1. Case study periods and plume identification

Fig. 5 illustrates the time series of the OC, EC, inorganic ions and gas-phase pollutants during the study periods in summer and autumn when several photochemical episodes were observed with
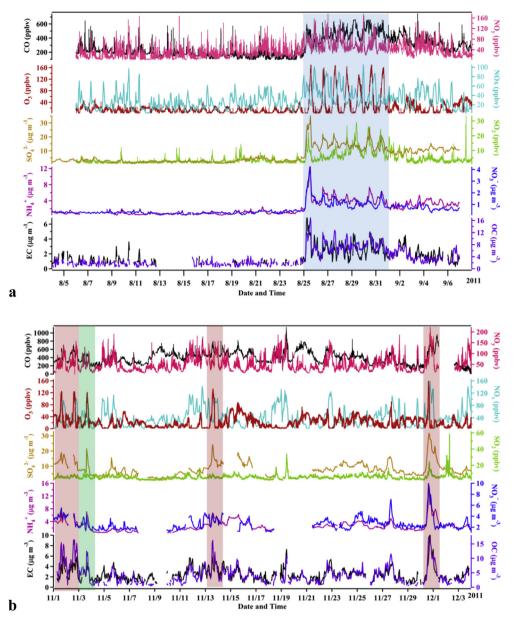
Fig. 4. Correlations between the SOC and odd oxygen ($O_x = O_3 + NO_2$) colored by time of day in (**a**) summer (August, 2011) and (**b**) autumn (November, 2011) in TC site.

Fig. 5. Time series of OC, EC, inorganic aerosol composition and gas-phase pollutants in **(a)** August 2011 and **(b)** November 2011 at TC. The shaded regions represent the case-study periods in the text.
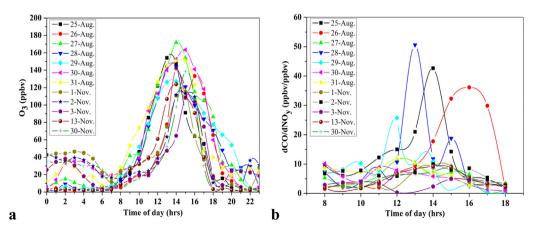

Fig. 6. (a) Diurnal variations of O_3 observed at TC during the smoggy days with hourly averaged O_3 concentrations exceeding 100 ppbv. **(b)** Daytime variations of the "24 hourly" dCO/dNO_y ratios at TC during the smoggy days.

the hourly averaged maximum O_3 concentrations of over 100 ppbv (Fig. 6a). Elevated OC, EC and inorganic ion concentrations were also observed during these episodes, shown as the shaded regions in Fig. 5.

To identify the origins of the plumes at TC during the photochemical episodes, two methods (i.e., chemical tracer and back trajectory analysis) were adopted, which are similar to those described by Zhang et al. (2007a). Wang et al. (2003) showed large differences in CO/NO_y emission ratios between the PRD cities and Ho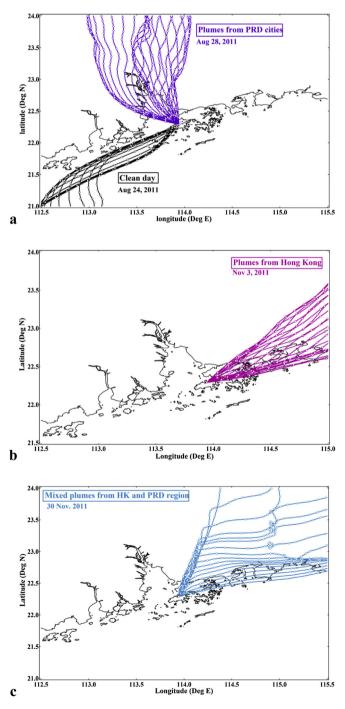ng Kong (i.e., CO/NO_y ratio>20 ppbv ppbv^{-1} in the PRD plumes but about 3.9–6 ppbv ppbv^{-1} in the Hong Kong plumes). Following the approach of Zhang et al. (2007a), we calculated "24 hourly" dCO/dNO_y ratio (dCO = the measured 1-h averaged CO concentrations subtracted the minimum CO concentration that day; dNO_y = the measured 1-h averaged NO_y concentrations subtracted the minimum NO_y concentration that day). Fig. 6b shows the daytime variations of the dCO/dNO_y ratios during the aforementioned photochemical episodes. Back trajectories were used to check the validity of the chemical tracer method (dCO/dNO_y ratios). The back trajectories were calculated using the NOAA/ARL HYSPLIT 4.9 model driven by the GDAS meteorological data (Draxler and Rolph, 2003). Fig. 7 shows the representative types of air masses on August 28, November 3 and November 30, 2011. Despite the coarse resolution of the GDAS data (i.e., 1° × 1°), the back trajectories generally verified the results from the dCO/dNO_y ratios, that is, the cases of high CO/NO_y ratios corresponded to air masses from the inland PRD region. Using the above methods, we classified the photochemical events in summer and autumn as HK, the PRD, and mixed HK and the PRD (see Table 2), and these events are subject to further analysis.

3.3.2. Photochemical evolution of OA in urban plumes

We next calculate the SOC production rates in the identified photochemical episodes. The SOC concentrations were normalized by the excess CO (the measured CO concentrations minus the background CO concentration) in order to reduce the influence of dilution (Kleinman et al., 2008). In this study, the background CO concentrations were obtained from a background Hok Tsui (HT) monitoring station, which is located on the southeastern tip of Hong Kong Island and is considered as the background site of Hong Kong. An examination of the CO data at HT in August and November 2011 indicated absence of a typical double-peak pattern for an urban site but only slightly higher daytime concentrations, confirming only small influence from urban sources on HT (figures not shown). The background CO was the average concentration in the "Marine" air group in August and "Aged continental" air mass in November, as these two air masses arriving at HT were from long distant sources in the respective months (Wang et al., 2009). Using this approach, the background CO concentration was 92 and 186 ppbv in August and November 2011, respectively.

Fig. 8 shows the ΔCO-normalized SOC as a function of the photochemical age on the episode days. The normalized SOC concentrations increased with the increase in photochemical age, indicating that SOC was produced as the plume advected to the TC site. The estimated aging time in late summer was less than 6 h, much shorter than the times of urban plumes observed in other downwind sites: ∼24 h in Mexico City in spring (Kleinman et al., 2008), 15 h in Ontario in summer (Slowik et al., 2011), and 12 h in Tokyo in summer (Miyakawa et al., 2008). This can be partly explained by a more approximation of the TC site to urban areas as

Fig. 7. Back trajectories of the air masses arriving at TC on **(a)** August 28, 2011, **(b)** November 3, 2011 and **(c)** November 30, 2011.

Table 2
Time period, air mass categorization, and SOC production of pollution episodes in summer and autumn.

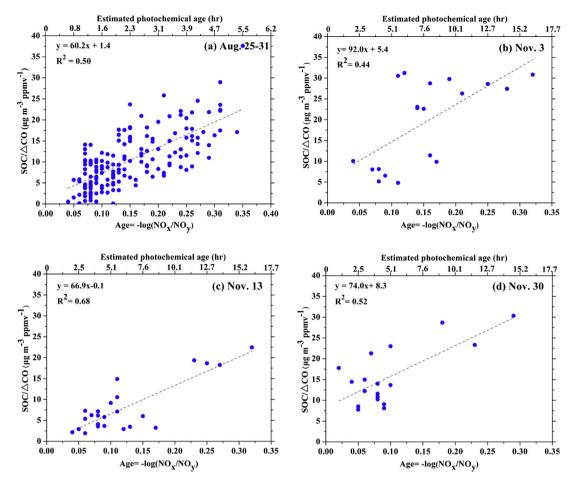| Date	Daily maximum 1-h O_3 concentration (ppbv)	Air mass categorization	Aging time (h)	SOC production rate (μg m^{-3} ppmv^{-1} h^{-1})
Aug. 25–31	127.2–171.7	The PRD	5.5	3.86
Nov. 1–2	115.4	Mixed HK and the PRD	13.9	1.31
Nov. 3	108.4	HK	15.9	1.82
Nov. 13	123.9	Mixed HK and the PRD	16.4	1.32
Nov. 30	138.5	Mixed HK and the PRD	14.7	1.46

Fig. 8. ΔCO-normalized SOC concentrations (SOC/ΔCO) as a function of photochemical age ($-\log_{10}(NO_x/NO_y)$) during the polluted periods: **(a)** August 25–31, 2011, plumes from the PRD cities; **(b)** November 3, 2011, plumes from Hong Kong and **(c)** and **(d)** plumes from both the PRD cities and Hong Kong on November 13 and 30, 2011.

compared to other downwind sites. The slopes of SOC/ΔCO versus estimated photochemical age (hours) are the SOC production rates, which varied slightly among the three types of air masses at TC (Fig. 8 and Table 2).

We first considered the urban plumes from the PRD cities observed during the multi-day episode (August 25–31). The slope of the SOC/ΔCO versus $-\log_{10}(NO_x/NO_y)$ was 60.2 μg m^{-3} ppmv^{-1}. Assuming a factor of 1.6 to convert SOC to SOA (Turpin and Lim, 2001), the slope is 96.3 μg m^{-3} ppmv^{-1}, which is comparable with that observed in the Mexico City outflow (71.4 μg m^{-3} ppmv^{-1}) (Kleinman et al., 2008), but much lower than that measured downwind Detroit/Winsor in Canada (189.2 μg m^{-3} ppmv^{-1}) (Slowik et al., 2011). Using the more conventional time scale (hour), the average SOC production rate was 3.86 μg m^{-3} ppmv^{-1} h^{-1} for PRD plumes (with a SOA production rate of about

6.18 μg m^{-3} ppmv^{-1} h^{-1}). For the mixed plumes from HK and the PRD, the slopes of SOC/ΔCO versus $-\log_{10}(NO_x/NO_y)$ varied from 66.2 to 74.0 μg m^{-3} ppmv^{-1}. The corresponding SOC production rates ranged from 1.31 to 1.46 μg m^{-3} ppmv^{-1} h^{-1}. For the case on November 3, 2011, when the plume was largely of local (Hong Kong) origin, the slope of SOC/ΔCO versus $-\log_{10}(NO_x/NO_y)$ was 92.0 μg m^{-3} ppmv^{-1} and the SOC production rate was 1.82 μg m^{-3} ppmv^{-1} h^{-1}. The extent of production of organic aerosols from urban Hong Kong to the receptor site could also be illustrated by comparing the SOC observed at TC (the receptor) with that at an urban site in Hong Kong in autumn 2010 (PolyU site, Fig. 1). The daytime contribution of SOC to the OC at the receptor site was higher (41.0%) than that at PolyU site (31.3%), indicating that the aerosols had become more aged due to photochemical processing during their transport from Hong Kong downtown to the downwind TC site.

In summary, the SOA production rate of 6.18 μg m^{-3} ppmv^{-1} h^{-1} in Hong Kong during the summer multi-day episode is at the high end of the range ($\sim$2–5 μg m^{-3} ppmv^{-1} h^{-1}) reported in Mexico City, the eastern U.S. and Pasadena in California (DeCarlo et al., 2010; Hayes et al., 2013), while the rates in autumn are in the low end of the reported range, possibly due to reduced photochemical activity in autumn season.

3.3.3. Microscopic characterization of organic aerosols aging in the PRD outflow

To provide more information on the aging of organic aerosols in the PRD outflow, we analyzed the microscopic data of individual aerosol particles obtained from the high-resolution TEM. The
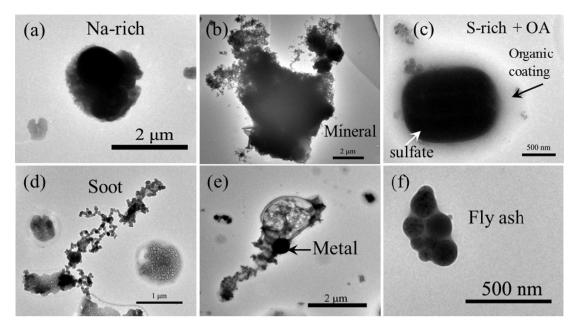
Table 3
Sampling time and atmospheric conditions of individual aerosol particle samples at TC.

Date	Start time	End time	RH (%)	Temp. (°C)	WD	WS (m s^{-1})	PM$_{2.5}$ (μg m^{-3})	O$_3$ (ppbv)
Clean day								
2011/8/24	13:56	14:01	51%	36.5	E	1.6	11.0	35.1
2011/8/24	17:27	17:32	60%	35.0	W	1.5	7.8	23.3
Smoggy days								
2011/8/25	10:13	10:15	71%	33.8	NNW	1.5	72.0	37.0
2011/8/25	18:56	18:59	68%	31.9	N	0.6	33.5	4.0
2011/8/27	12:15	12:16	57%	34.9	NW	2.6	95.0	104.0
2011/8/31	17:47	17:48	56%	34.2	NW	2.4	78.4	55.0

Fig. 9. TEM images of six types of individual particles collected on August 24–31, 2011: **(a)** Na-rich, **(b)** mineral, **(c)** sulfate and organic aerosols, **(d)** soot, **(e)** metal and **(f)** fly ash. The compositions of the individual aerosol particles were determined by TEM/EDS.
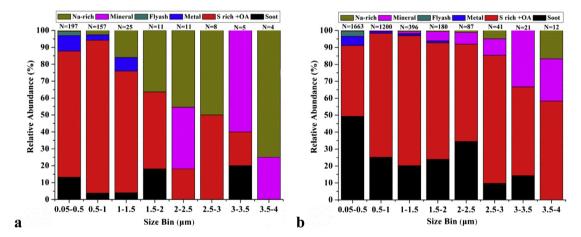

Fig. 10. The proportions of different aerosol particle types (Na-rich, mineral, fly ash, metal, sulfate and organic aerosols (S rich + OA), and soot) in different size ranges for **(a)** the clean day and **(b)** the smoggy days in summer (see in Table 3).
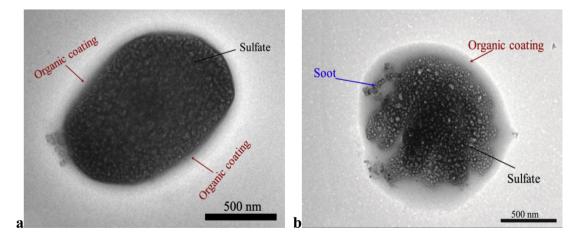

Fig. 11. **(a)** Thin organic coating on the clean day (Aug. 24, 2011). **(b)** Thick organic coating on the smoggy day (Aug. 25, 2011).

particles were collected during one clean day and three smoggy days in August 2011 (Table 3). A total of 4018 particles from 6 samples (2 on clean day and 4 on smoggy days) were examined, and six types of individual particles were obtained, including Na-rich, mineral, fly ash, metal, sulfate/organics, and soot particles (Fig. 9). On the clean day, the particle diameters were mostly lower than 1.5 μm in size, and the sulfates and organics comprised about 80% of the total individual particles (Fig. 10a). On the smoggy days, the sulfate and organics had a wider range of diameters compared with those on the clean day, and sulfate and organics were the main components even in the coarse mode (up to 4 μm) (Fig. 10b). The results suggest that the aerosols on the smoggy days were subjected to intensive processing (i.e., photochemical oxidation, coagulation and heterogeneous nucleation), resulting in an enrichment of secondary materials in coarse particles. In addition to the presence of sulfate and organics in larger-size particle, the organic coatings on the sulfate were much thinker on smoggy days (e.g., Fig. 11b) than on the clean day (e.g., Fig. 11a). Organics coatings on sulfate particles have been considered as SOA (Li and Shao, 2010), and the thinker organic coatings on smoggy days imply more SOA than on the clean day, which is consistent with SOC concentration from the real-time measurements (1.32 μg m^{-3} on clean days versus 3.58 μg m^{-3} on the smoggy days in August 2011). The morphology data indicate that organics were totally internally mixed with sulfate particles in chemically processed air, highlighting the complexity in understanding and predicting the chemical processes and optical properties of aerosol of different ageing.

4. Summary

OC, EC, PM$_{2.5}$ and other gaseous and particulate pollutants were measured at a receptor site in Hong Kong in August, November, February and May during the year of 2011–2012. Clear seasonal and diurnal variations of organic aerosols were observed, with the highest OC concentrations in autumn. The estimated SOC concentrations were 2.14, 1.85, 1.91 and 1.09 μg m^{-3}, accounting for 40.7%, 36.8%, 50.1% and 60.2% of the total OC in summer, autumn, winter and spring, respectively. The SOC and odd oxygen (O$_x$) were highly correlated during the summer and autumn seasons, suggesting that photochemical processing might have contributed to the formation of organic aerosols.

The photochemical aging of organic aerosol was quantitatively studied during the smog episodes in summer and autumn. The results showed that the PRD cities and Hong Kong were the source regions and that aerosol particles became more aged as they were advected toward the receptor TC site. The SOC production rates were estimated to be in the range of 1.31–1.82 μg m^{-3} ppmv^{-1} h^{-1} in autumn and 3.86 μg m^{-3} ppmv^{-1} h^{-1} in summer, with the summer rate in the upper end of the range observed in the U.S. and Mexico City. The reduced rates in the autumn episodes may be due to decreased level of photochemistry. TEM images revealed organic coatings on the sulfates and soot in all particle sizes (0.05–4.0 μm) during the episodes, indicating complex physico-chemical processing of organic aerosols. The results of this study can help improve modeling the formation of organic aerosols in polluted sub-tropical environments.

Disclaimer

The opinions expressed in this paper are those of the authors and do not necessarily reflect the views or policies of the Government of the Hong Kong Special Administrative Region, nor does mention of trade names or commercial products constitute an endorsement or recommendation of their use.

References

Andreae, M.O., Schmid, O., Yang, H., Chand, D., Zhen Yu, J., Zeng, L.M., Zhang, Y.H., 2008. Optical properties and chemical composition of the atmospheric aerosol in urban Guangzhou, China. Atmos. Environ. 42 (25), 6335–6350.

Bahreini, R., Ervens, B., Middlebrook, A., Warneke, C., de Gouw, J., DeCarlo, P., Jimenez, J., Brock, C., Neuman, J., Ryerson, T., 2009. Organic aerosol formation in urban and industrial plumes near Houston and Dallas, Texas. J. Geophys. Res. Atmos. 114, D00F16. http://dx.doi.org/10.1029/2008JD011493.

Bond, T.C., Doherty, S.J., Fahey, D.W., Forster, P.M., Berntsen, T., DeAngelo, B.J., Flanner, M.G., Ghan, S., Kärcher, B., Koch, D., Kinne, S., Kondo, Y., Quinn, P.K., Sarofim, M.C., Schultz, M.G., Schulz, M., Venkataraman, C., Zhang, H., Zhang, S., Bellouin, N., Guttikunda, S.K., Hopke, P.K., Jacobson, M.Z., Kaiser, J.W., Klimont, Z., Lohmann, U., Schwarz, J.P., Shindell, D., Storelvmo, T., Warren, S.G., Zender, C.S., 2013. Bounding the role of black carbon in the climate system: a scientific assessment. J. Geophys. Res. Atmos. 118. http://dx.doi.org/10.1002/jgrd.50171.

Cao, J., Lee, S., Ho, K., Zou, S., Fung, K., Li, Y., Watson, J., Chow, J., 2004. Spatial and seasonal variations of atmospheric organic carbon and elemental carbon in Pearl River Delta Region, China. Atmos. Environ. 38 (27), 4447–4456.

Chan, C.K., Yao, X., 2008. Air pollution in mega cities in China. Atmos. Environ. 42 (1), 1–42.

Cheng, Y., Lee, S.C., Ho, K.F., Chow, J.C., Watson, J.G., Louie, P.K.K., Cao, J.J., Hai, X., 2010. Chemically-speciated on-road PM2.5 motor vehicle emission factors in Hong Kong. Sci. Total Environ. 408 (7), 1621–1627.

Cheng, Y.F., Eichler, H., Wiedensohler, A., Heintzenberg, J., Zhang, Y.H., Hu, M., Herrmann, H., Zeng, L.M., Liu, S., Gnauk, T., Brüggemann, E., He, L.Y., 2006. Mixing state of elemental carbon and non-light-absorbing aerosol components derived from in situ particle optical properties at Xinken in Pearl River Delta of China. J. Geophys. Res. Atmos. 111, D20204. http://dx.doi.org/10.1029/22005JD006929.

De Gouw, J., Brock, C., Atlas, E., Bates, T., Fehsenfeld, F., Goldan, P., Holloway, J., Kuster, W., Lerner, B., Matthew, B., 2008. Sources of particulate matter in the northeastern United States in summer: 1. Direct emissions and secondary formation of organic matter in urban plumes. J. Geophys. Res. Atmos. 113, D08301. http://dx.doi.org/10.1029/02007JD009243.

DeCarlo, P., Ulbrich, I., Crounse, J., de Foy, B., Dunlea, E., Aiken, A., Knapp, D., Weinheimer, A., Campos, T., Wennberg, P., 2010. Investigation of the sources and processing of organic aerosol over the Central Mexican Plateau from aircraft measurements during MILAGRO. Atmos. Chem. Phys. 10 (12), 5257–5280.

Ding, X., Wang, X.-M., Gao, B., Fu, X.-X., He, Q.-F., Zhao, X.-Y., Yu, J.-Z., Zheng, M., 2012. Tracer-based estimation of secondary organic carbon in the Pearl River Delta, south China. J. Geophys. Res. Atmos. 117, D05313. http://dx.doi.org/10.1029/02011JD016596.

Draxler, R., Rolph, G., 2003. HYSPLIT (HYbrid Single-particle Lagrangian Integrated Trajectory) Model. NOAA Air Resources Laboratory, Silver Spring, MD. Access via NOAA ARL READY Website. http://www.arl.noaa.gov/ready/hysplit4.html.

Dzepina, K., Cappa, C.D., Volkamer, R.M., Madronich, S., DeCarlo, P.F., Zaveri, R.A., Jimenez, J.L., 2010. Modeling the multiday evolution and aging of secondary organic aerosol during MILAGRO 2006. Environ. Sci. Technol. 45 (8), 3496–3503.

Gao, X., Xue, L., Wang, X., Wang, T., Yuan, C., Gao, R., Zhou, Y., Nie, W., Zhang, Q., Wang, W., 2012. Aerosol ionic components at Mt. Heng in central southern China: abundances, size distribution, and impacts of long-range transport. Sci. Total Environ. 433, 498–506.

Gnauk, T., Muller, K., van Pinxteren, D., He, L.Y., Niu, Y., Hu, M., Herrmann, H., 2008. Size-segregated particulate chemical composition in Xinken, Pearl River Delta, China: OC/EC and organic compounds. Atmos. Environ. 42 (25), 6296–6309.

Hagler, G., Bergin, M., Salmon, L., Yu, J., Wan, E., Zheng, M., Zeng, L., Kiang, C., Zhang, Y., Lau, A., 2006. Source areas and chemical composition of fine particulate matter in the Pearl River Delta region of China. Atmos. Environ. 40 (20), 3802–3815.

Hayes, P.L., Ortega, A.M., Cubison, M.J., Froyd, K.D., Zhao, Y., Cliff, S.S., Hu, W.W., Toohey, D.W., Flynn, J.H., Lefer, B.L., Grossberg, N., Alvarez, S., Rappenglück, B., Taylor, J.W., Allan, J.D., Holloway, J.S., Gilman, J.B., Kuster, W.C., de Gouw, J.A., Massoli, P., Zhang, X., Liu, J., Weber, R.J., Corrigan, A.L., Russell, L.M., Isaacman, G., Worton, D.R., Kreisberg, N.M., Goldstein, A.H., Thalman, R., Waxman, E.M., Volkamer, R., Lin, Y.H., Surratt, J.D., Kleindienst, T.E., Offenberg, J.H., Dusanter, S., Griffith, S., Stevens, P.S., Brioude, J., Angevine, W.M., Jimenez, J.L., 2013. Organic aerosol composition and sources in Pasadena,

California during the 2010 CalNex campaign. J. Geophys. Res. Atmos. 118. http://dx.doi.org/10.1002/jgrd.50530.

Hu, D., Bian, Q., Lau, A.K.H., Yu, J.Z., 2010. Source apportioning of primary and secondary organic carbon in summer PM2. 5 in Hong Kong using positive matrix factorization of secondary and primary organic tracer data. J. Geophys. Res. Atmos. 115, D16204. http://dx.doi.org/10.1029/12009JD012498.

Hu, W.W., Hu, M., Deng, Z.Q., Xiao, R., Kondo, Y., Takegawa, N., Zhao, Y.J., Guo, S., Zhang, Y.H., 2012. The characteristics and origins of carbonaceous aerosol at a rural site of PRD in summer of 2006. Atmos. Chem. Phys. 12 (4), 1811—1822.

Huang, X.F., Yu, J., He, L.Y., Yuan, Z., 2006. Water-soluble organic carbon and oxalate in aerosols at a coastal urban site in China: size distribution characteristics, sources and formation mechanisms. J. Geophys. Res. Atmos. 111, D22212. http://dx.doi.org/10.1029/22006JD007408.

Jimenez, J., Canagaratna, M., Donahue, N., Prevot, A., Zhang, Q., Kroll, J.H., DeCarlo, P.F., Allan, J.D., Coe, H., Ng, N., 2009. Evolution of organic aerosols in the atmosphere. Science 326 (5959), 1525—1529.

Johnson, D., Utembe, S., Jenkin, M., Derwent, R., Hayman, G., Alfarra, M., Coe, H., McFiggans, G., 2006. Simulating regional scale secondary organic aerosol formation during the TORCH 2003 campaign in the southern UK. Atmos. Chem. Phys. 6 (2), 403—418.

Kleinman, L., Springston, S., Daum, P., Lee, Y.-N., Nunnermacker, L., Senum, G., Wang, J., Weinstein-Lloyd, J., Alexander, M., Hubbe, J., 2008. The time evolution of aerosol composition over the Mexico City plateau. Atmos. Chem. Phys. 8, 1559—1575.

Lee, B.P., Li, Y.J., Yu, J.Z., Louie, P.K.K., Chan, C.K., 2013. Physical and chemical characterization of ambient aerosol by HR-ToF-AMS at a suburban site in Hong Kong during springtime 2011. J. Geophys. Res. Atmos. 118 (15), 8625—8639.

Li, W., Shao, L., 2010. Mixing and water-soluble characteristics of particulate organic compounds in individual urban aerosol particles. J. Geophys. Res. Atmos. 115 (D2). http://dx.doi.org/10.1029/2009JD012575.

Li, W., Wang, T., Zhou, S., Lee, S., Huang, Y., Gao, Y., Wang, W., 2013. Microscopic observation of metal-containing particles from Chinese Continental outflow observed from a non-industrial site. Environ. Sci. Technol. 47 (16), 9124—9131.

Lim, H.J., Turpin, B.J., 2002. Origins of primary and secondary organic aerosol in Atlanta: results of time-resolved measurements during the Atlanta supersite experiment. Environ. Sci. Technol. 36 (21), 4489—4496.

Miyakawa, T., Takegawa, N., Kondo, Y., 2008. Photochemical evolution of submicron aerosol chemical composition in the Tokyo megacity region in summer. J. Geophys. Res. Atmos. 113, D14304. http://dx.doi.org/10.1029/12007JD009493.

Miyazaki, Y., Kondo, Y., Shiraiwa, M., Takegawa, N., Miyakawa, T., Han, S., Kita, K., Hu, M., Deng, Z., Zhao, Y., 2009. Chemical characterization of water-soluble organic carbon aerosols at a rural site in the Pearl River Delta, China, in the summer of 2006. J. Geophys. Res. Atmos. 114, D14208. http://dx.doi.org/10.1029/12009JD011736.

Nel, A., 2005. Air pollution-related illness: effects of particles. Science 308 (5723), 804—806.

Robinson, A.L., Donahue, N.M., Shrivastava, M.K., Weitkamp, E.A., Sage, A.M., Grieshop, P.F., Lane, T.E., Pierce, J.R., Pandis, S.N., 2007. Rethinking organic aerosols: semivolatile emissions and photochemical aging. Science 315 (5816), 1259—1262.

Seinfeld, J., Pandis, S., 2006. Atmospheric Chemistry and Physics:From Air Pollution to Climate Change. John Wiley & Sons, New York.

Slowik, J.G., Brook, J., Chang, R.Y.W., Evans, G.J., Hayden, K., Jeong, C.H., Li, S.M., Liggio, J., Liu, P.S.K., McGuire, M., Mihele, C., Sjostedt, S., Vlasenko, A., Abbatt, J.P.D., 2011. Photochemical processing of organic aerosol at nearby continental sites: contrast between urban plumes and regional aerosol. Atmos. Chem. Phys. 11 (6), 2991—3006.

Turpin, B., Huntzicker, J., 1995. Identification of secondary organic aerosol episodes and quantitation of primary and secondary organic aerosol concentrations during SCAQS. Atmos. Environ. 29 (23), 3527—3544.

Turpin, B., Lim, H., 2001. Species contributions to PM2.5 mass concentrations: revisiting common assumptions for estimating organic mass. Aerosol Sci. Technol. 35 (1), 602—610.

Wang, T., Wu, Y., Cheung, T., Lam, K., 2001. A study of surface ozone and the relation to complex wind flow in Hong Kong. Atmos. Environ. 35 (18), 3203—3215.

Wang, T., Poon, C., Kwok, Y., Li, Y., 2003. Characterizing the temporal variability and emission patterns of pollution plumes in the Pearl River Delta of China. Atmos. Environ. 37 (25), 3539—3550.

Wang, T., Wei, X.L., Ding, A.J., Poon, C.N., Lam, K.S., Li, Y.S., Chan, L.Y., Anson, M., 2009. Increasing surface ozone concentrations in the background atmosphere of Southern China, 1994—2007. Atmos. Chem. Phys. 9 (16), 6217—6227.

Wang, Z., Wang, T., Gao, R., Xue, L., Guo, J., Zhou, Y., Nie, W., Wang, X., Xu, P., Gao, J., 2011. Source and variation of carbonaceous aerosols at Mount Tai, North China: results from a semi-continuous instrument. Atmos. Environ. 45 (9), 1655—1667.

Wang, Z., Wang, T., Guo, J., Gao, R., Xue, L., Zhang, J., Zhou, Y., Zhou, X., Zhang, Q., Wang, W., 2012. Formation of secondary organic carbon and cloud impact on carbonaceous aerosols at Mount Tai, North China. Atmos. Environ. 46, 516—527.

Weber, R., Sullivan, A., Peltier, R., Russell, A., Yan, B., Zheng, M., De Gouw, J., Warneke, C., Brock, C., Holloway, J., 2007. A study of secondary organic aerosol formation in the anthropogenic-influenced southeastern United States. J. Geophys. Res. Atmos. 112, D13302. http://dx.doi.org/10.1029/12007JD008408.

Xiao, R., Takegawa, N., Kondo, Y., Miyazaki, Y., Miyakawa, T., Hu, M., Shao, M., Zeng, L.M., Hofzumahaus, A., Holland, F., Lu, K., Sugimoto, N., Zhao, Y., Zhang, Y.H., 2009. Formation of submicron sulfate and organic aerosols in the outflow from the urban region of the Pearl River Delta in China. Atmos. Environ. 43 (24), 3754—3763.

Xu, Z., Wang, T., Xue, L.K., Louie, P.K.K., Luk, C.W.Y., Gao, J., Wang, S.L., Chai, F.H., Wang, W.X., 2013. Evaluating the uncertainties of thermal catalytic conversion in measuring atmospheric nitrogen dioxide at four differently polluted sites in China. Atmos. Environ. 76, 221—226.

Yu, H., Wu, C., Wu, D., Yu, J., 2010. Size distributions of elemental carbon and its contribution to light extinction in urban and rural locations in the Pearl River delta region, China. Atmos. Chem. Phys. 10 (11), 5107—5119.

Yu, J., Tung, J., Wu, A., Lau, A., Louie, P., Fung, J., 2004. Abundance and seasonal characteristics of elemental and organic carbon in Hong Kong PM10. Atmos. Environ. 38 (10), 1511—1521.

Yuan, Z.B., Yu, J.Z., Lau, A.K.H., Louie, P.K.K., Fung, J.C.H., 2006. Application of positive matrix factorization in estimating aerosol secondary organic carbon in Hong Kong and its relationship with secondary sulfate. Atmos. Chem. Phys. 6 (1), 25—34.

Zhang, J., Wang, T., Chameides, W., Cardelino, C., Kwok, J., Blake, D., Ding, A., So, K., 2007a. Ozone production and hydrocarbon reactivity in Hong Kong, Southern China. Atmos. Chem. Phys. 7, 557—573.

Zhang, Q., Jimenez, J., Canagaratna, M., Allan, J., Coe, H., Ulbrich, I., Alfarra, M., Takami, A., Middlebrook, A., Sun, Y., 2007b. Ubiquity and dominance of oxygenated species in organic aerosols in anthropogenically-influenced Northern Hemisphere midlatitudes. Geophys. Res. Lett. 34, L13801. http://dx.doi.org/10.1029/12007GL029979.

Zhang, X., Wang, Y., Zhang, X., Guo, W., Gong, S., 2008a. Carbonaceous aerosol composition over various regions of China during 2006. J. Geophys. Res. Atmos. 113, D14111. http://dx.doi.org/10.1029/12007JD009525.

Zhang, Y., Hu, M., Zhong, L., Wiedensohler, A., Liu, S., Andreae, M., Wang, W., Fan, S., 2008b. Regional integrated experiments on air quality over Pearl River Delta 2004 (PRIDE-PRD2004): overview. Atmos. Environ. 42 (25), 6157—6173.

Zheng, M., Wang, F., Hagler, G., Hou, X., Bergin, M., Cheng, Y., Salmon, L., Schauer, J.J., Louie, P.K.K., Zeng, L., 2011. Sources of excess urban carbonaceous aerosol in the Pearl River Delta Region, China. Atmos. Environ. 45 (5), 1175—1182.

Zhong, L., Louie, P.K.K., Zheng, J., Yuan, Z., Yue, D., Ho, J.W.K., Lau, A.K.H., 2013. Science-policy interplay: air quality management in the Pearl River Delta region and Hong Kong. Atmos. Environ. 76, 3—10.